



OPEN ACCESS

EDITED BY

Philip J Erickson,
Massachusetts Institute of Technology,
United States

REVIEWED BY

Shican Qiu,
Chang'an University, China
Chris Deacon,
University of Bath, United Kingdom

*CORRESPONDENCE

Vania F. Andrioli,
✉ vania.andrioli@inpe.br

RECEIVED 10 December 2024

ACCEPTED 02 April 2025

PUBLISHED 23 April 2025

CITATION

Andrioli VF, Xu J, Batista PP, Resende LCA, Santos AM, Olajide-Owoyomi F, Pimenta AA, Martins MPP, Da Silva LA, Moro J, de Jesus R, Yang G, Wang C and Liu Z (2025) Fast-type sporadic Na and K layers over São José dos campos, Brazil, and their link to meteor ablation.

Front. Astron. Space Sci. 12:1542596.
doi: 10.3389/fspas.2025.1542596

COPYRIGHT

© 2025 Andrioli, Xu, Batista, Resende, Santos, Olajide-Owoyomi, Pimenta, Martins, Da Silva, Moro, de Jesus, Yang, Wang and Liu. This is an open-access article distributed under the terms of the [Creative Commons Attribution License \(CC BY\)](https://creativecommons.org/licenses/by/4.0/). The use, distribution or reproduction in other forums is permitted, provided the original author(s) and the copyright owner(s) are credited and that the original publication in this journal is cited, in accordance with accepted academic practice. No use, distribution or reproduction is permitted which does not comply with these terms.

Fast-type sporadic Na and K layers over São José dos campos, Brazil, and their link to meteor ablation

Vania F. Andrioli^{1,2,3*}, Jiyao Xu¹, Paulo P. Batista², Laysa C. A. Resende^{1,2,3}, Angela M. Santos^{1,2,3}, Femi Olajide-Owoyomi², Alexandre A. Pimenta², Maria P. P. Martins², Ligia A. Da Silva^{1,2,3}, Juliano Moro^{1,2,3}, Rodolfo de Jesus², Guotao Yang^{1,3}, Chi Wang¹ and Zhengkuan Liu^{1,3}

¹State Key Laboratory for Space Weather, National Space Science Center, Chinese Academy of Sciences, Beijing, China, ²Division of Heliophysics, Planetary Science, and Aeronomy (DIHPA), National Institute for Space Research (INPE), São José dos Campos, Brazil, ³China-Brazil Joint Laboratory for Space Weather, NSSC/INPE, São José dos Campos, Brazil

This study utilizes 3 years of observational data from the China-Brazil Joint Laboratory for Space Weather (CBJLSW) dual-beam Na-K LIDAR to investigate fast-type sporadic sodium (Na) and potassium (K) layers. The focus is on the sudden enhancement of these metal densities within thin layers, the duration of which is less than 1 hour. These transient layers were identified in five nights of observational data and were always located a few hundred meters above the main Na and K layers. There was a good correspondence between the fast-type Ns layer and the occurrence of the Sporadic-E (Es) layer, which also presented a short time of duration. Moreover, the results show an increase in the meteor rate during these Ns layers' time and altitudinal range. Our analysis aims to elucidate the formation mechanisms of these fast-type neutral sporadic layers. The slightly higher peak altitudes and earlier started time observed in the Na layer compared to K are evidence of the link to differential meteor ablation. Additionally, the different values found in the relative abundance of the Na to K ratio between the Ns and background layers indicate an extra input of metals in the layers instead of a vertical redistribution of the pre-existing metal normal layer. The findings suggest that the formation of the fast-type Ns layers is linked to the direct deposition of these metals by meteor ablation.

KEYWORDS

Na sporadic layer, K sporadic layer, sporadic E layer, meteor ablation, billow-like structures

1 Introduction

Several authors have investigated the sudden sporadic enhancement of neutral metal atom concentration within narrow layers (see [Mathews et al., 1993](#); [Clemesha \(1995\)](#); [Cox and Plane \(1998\)](#); [Raizada et al. \(2015\)](#)). The first observation of such an event was reported by [Clemesha et al. \(1978\)](#), using a Na LIDAR in São José dos Campos, Brazil. [Clemesha \(1995\)](#) performed a review of the studies on Sporadic Neutral metal

layers, called the Ns layer, in analogy with ionospheric Sporadic E (Es) layers. Following this convention, we adopt the same terminology in the present paper. The Ns layers are typically superimposed on a nearly constant background layer of the same metal, extending from approximately 80 km–105 km and exhibiting a roughly Gaussian shape (Clemesha, 1995). Numerous studies have been conducted to characterize better and understand the Ns layers (e.g., Batista et al. (1989); Clemesha (1995); Cox and Plane (1998); Jiao et al. (2015); Raizada et al. (2015); Andrioli et al. (2021)). These works have helped us identify several key characteristics of the Ns layers, such as their concentration being between 2 and 20 times higher than the background layer. The vertical extent of the Ns layers ranges from a few hundred to several thousand meters, and their duration lasts between a few minutes and many hours. Regarding their horizontal extension, the literature contains few studies; estimates range from 100–500 km (Batista et al., 1991) to approximately 1,000 km (Kane et al., 1991). Therefore, the main characteristics include a small vertical extent, a concentration at least twice that of the local background, and rapid growth, even though researchers have also used other criteria to define Ns layers.

Concerning the formation mechanism of the Ns layers, the current theories proposed can be divided into three categories: (i) the injection of fresh atomic metals through meteoric ablation, (ii) the vertical redistribution of atomic metals from the background layer, and (iii) the *in-situ* production of atomic metals from a reservoir species. In their first observation of the Ns layer, Clemesha et al. (1978) suggested that excess sodium atoms likely originated from meteor deposition. On the other hand, Clemesha et al. (1988) proposed a mechanism in which wind shear could convert an initial thick layer caused by meteor deposition into a thinner one. However, based on the large horizontal extension measured mainly by Kane et al. (1991), such a mechanism requires an unreasonably large mass of meteor to explain the observed events (Clemesha, 1995). Recently, Pimenta et al. (2022) reported a case study in which a meteor disintegration was observed in the airglow (NaD) imager, with dimensions of 35.6 km × 9.18 km and an average velocity of approximately 90 m⁻¹. This event was attributed as a possible source for the Ns layer observed in Na LIDAR, located about 180 km from the meteor observation. About the second category, being proposed by Clemesha (1995) to be the major generation mechanisms of Ns layers, the strong and abrupt increase in the total column abundance of these metals during some events shows that this mechanism cannot explain that specific type of Ns event, as reported by Andrioli et al. (2024). Lastly, the third one, *in-situ* production from a reservoir species, has been used to explain several case studies. In fact, the reservoir is usually linked to the Es layers since several authors presented a high correlation between Ns and Es layers [e.g., Clemesha et al. (1980); Batista et al., 1989; Kane et al., 1993; Mathews et al., 1993; Clemesha, 1995; Delgado et al., 2012]. This feature provides evidence for the ion-molecular neutralization mechanism as a source of the Ns layers, as proposed by Cox and Plane (1998). However, the main issue with this mechanism is the different abundance of metal ions in the Es layer compared to the Ns ones (~10%, in the case of Na⁺, as discussed by Clemesha et al., 1999), which limits its effectiveness in producing significant amounts of neutral sodium.

Despite all these experimental works and theoretical models, no single mechanism can explain all these characteristics of the Ns

layers. Some recent works (e.g., Jiao et al., 2015; Andrioli et al., 2021), based on simultaneous observations of Na and K species, revealed that even though Na and K are both alkali metals, their layers' morphology and Ns had different behaviors and characteristics. Thus, we believe in multiple mechanisms explaining the different "types" of Ns layers. As there is still no official classification for the different types of Ns layers, we suggest that the characteristics of Ns layers in the lidagrams can help to set about their formation mechanism. According to Andrioli et al. (2021), around 10% of Ns layers lasted less than 1 hour.

In the present study, we selected five cases from 185 nights of observations conducted between 2017 and 2019 to investigate short-duration Ns layers. These five events presented similar characteristics in the lidagram, were simultaneously observed in the Na and K layers, and lasted less than 1 hour. We refer to these cases as fast-type Ns layers. It is important to mention that these layers are distinct from the extremely thin, short-lived enhancements produced by meteor trains, which last only a few seconds (e.g., Von Zahn et al., 1999; Chu et al., 2000; Liu et al., 2014). The main objective of this work is to investigate those five very similar events and to explore their formation mechanism. We use three different instrumentation data to describe the phenomenon better: the CBJLSW Dual-beam Na-K LIDAR, the Digisonde, and the SKiYMET Meteor radar. In the following sections, we will present the method of analysis in Section 2, the results and discussion in Section 3, and finally, in Section 4, we provide compelling evidence establishing the connection between fast-type Ns layers and meteor ablation, as discussed in the conclusion.

2 Methodology

The narrow-band China-Brazil Joint Laboratory for Space Weather (CBJLSW) dual-beam Na-K LIDAR is installed at INPE's facilities in São José dos Campos (SJC, 23.1° S, 45.9° W), São Paulo, Brazil. This LIDAR uses two laser beams of 770 nm and 589 nm to simultaneously measure K and Na densities *via* the resonant scattering at the Mesosphere Lower Thermosphere (MLT) region. The Na and K photon counts are obtained with time and height resolution of 20 s and 96 m, respectively. We remove the background noise by using the average number of photon echoes received within the 120–130 km height range. In order to increase the signal-to-noise ratio (SNR) we combine 10 temporally consecutive profiles, with a resulting temporal resolution of 3.3 min when inferring Na and K densities within the MLT region. Using these enhanced profiles and applying the LIDAR Equation 1, Na/K concentrations ($N_{\text{Na/K}}$) profiles are obtained.

$$N_{\text{Na/K}}(r) = \frac{(n_{\text{Na/K}}(r) - n_B)\sigma_R(\text{Na/K})}{(n_R(r_R) - n_B)\sigma_{\text{eff}}(\text{Na/K})} \cdot \frac{4\pi N_R(r_R)r^2}{r_R^2} \quad (1)$$

Where r is the distance between scattering object and LIDAR receiving system, r_R is the reference height (~45 km), $n_{\text{Na/K}}$ is the photon counts of K or Na atoms, n_B is the respective photon count at the reference height, $N_R(r_R)$ is atmospheric number density at reference height from NRLMSISE-00 model, n_B is respective background noise of each wavelength, σ_{eff} is the effective fluorescence scattering cross-section of K or Na atoms and $\sigma_R(\text{Na/K})$ is the Rayleigh scattering cross-section for respective wavelength.

Scattering of aerosol particles can be neglected at these altitudes, optical thickness is less than 0.01; the line width of Na and K laser is ~ 1.473 GHz and 1.77 GHz, respectively; the effective scattering cross-section ($\sigma_{\text{eff}}(\text{Na/K})$) of Na and K atoms are $\sim 5.22 \times 10^{-16} \text{ m}^2 \text{ sr}^{-1}$ and $3.29 \times 10^{-17} \text{ m}^2 \text{ sr}^{-1}$, respectively (Du et al. (2021) and references therein).

The Digisonde installed at Cachoeira Paulista (CXP, 22.7° S, 45.0° W), which is located approximately 100 km from SJC, was used to observe the Es layer occurrence due to the unavailability of measurements from SJC. This sweeping frequency radar continuously transmits radio waves into the ionosphere in the range of 1–30 MHz, allowing for the measurement of several ionospheric parameters, such as virtual height, thickness, and critical frequency of the layers. The critical frequency is directly related to the maximum electron density of the different ionospheric layers. The data are recorded in ionograms, which are graphs of frequency *versus* virtual height plots, with a time resolution of 5, 10 or 15 min. For more details about the Digisonde see, for example, Reinisch et al., 2009.

The all-sky interferometric meteor radar, SKiYMET, also located in CXP, is used to analyze the meteor rate during the Ns occurrence. This system consists of a transmitting antenna that emits RF pulses at 35.24 MHz, with the echoes received by five receiving antennas. For each echo, the radial velocity, height, elevation, and azimuth are determined by the correlation between the signals from the various antennas and the pulse delay. This equipment is usually used to study horizontal wind from 80 to 100 km height, with a 2 km height and 1 h time resolutions, respectively. For more details on the system and methodology, see Hocking et al. (2001) and Batista et al. (2004). To investigate the meteor rate during the occurrence of fast-type Ns layers, we constructed histograms by counting meteors in 1 km altitude bins, integrated over the duration of each event. These counts were subsequently compared with the daily average, integrated over the same time interval.

3 Results and discussion

In the present work, we selected five events where we could observe the complete evolution of the fast-type Ns layer from observations of more than 1,500 h between 2017 and 2019. Table 1 shows the list of these events and their main characteristics, as observed in the lidargram and presented in Figures 1–5. The first column indicates the respective date followed by the time of their occurrence (started time: disrupted time) for the K and Na species, respectively. They all occurred after 02:00 UT, and the enhancement can be observed slightly earlier in the Na than in the K layer. Moreover, they last longer in Na than K, about 5 min on average. The time to reach maximum density indicates that K typically exhibits a shorter rise time than Na in most events. The peak height and the thickness of events observed in the Na layer are slightly higher and wider than registered in the K one. The last two columns represent their relative Na to K abundance ratio for the normal background (Nb) and inside the Ns layer. The Nb layers were built according to Andrioli et al. (2021), considering the time-averaged density of the entire corresponding date of observation and then integrating it in height to calculate the total column abundance for each constituent. Hence, the Nb layers' relative Na to

K abundance ratio is shown in the Rb column. In order to compare the relative amount corresponding to the Ns event, we calculate the column abundance considering only the height range where the fast enhancement of concentration was observed in the profile when the peak density is reached. The Na to K ratio for the Ns layer is shown in the Rs column. Except for 26 June 2019, where the same relative abundance ratio was found in the Rb and Rs, all others presented different values, demonstrating changes in the relative composition between the Nb and the Ns layers.

In the following figures we will present each one of the five events in their respective height-time-intensity plots of metal concentration, lidargrams. The concentrations of K and Na are displayed in the panels a) and b), respectively. We highlighted the studied Ns layers with a black circle. It is important to note that the events did not occur in isolation; each event exhibits additional weaker structures, connected to the main layer, which are marked by downward black arrows and resemble the billow-like structures previously observed in the Na layer in studies by Sridharan et al. (2009), and Sarkhel et al. (2012) and Sarkhel et al. (2015). These studies suggested that the billow-like structures could be generated by Kelvin–Helmholtz instability (KHI), which occurs in regions of strong wind shear. While the primary focus of this study is on the well-formed fast-type Ns layers, which are distinct from the main layer and identified by the black circle, the presence of these billow-like structures provides evidence of shear-induced instabilities, as will be discussed throughout this work. The parameters shown in Table 1 are obtained from the circled events. Note that they present similar shapes: all of them occurred at the top of the layer and were separated from the background layer, and also presented a rapid phase progression. This similar shape makes it possible to identify and separate these cases to be deeply investigated.

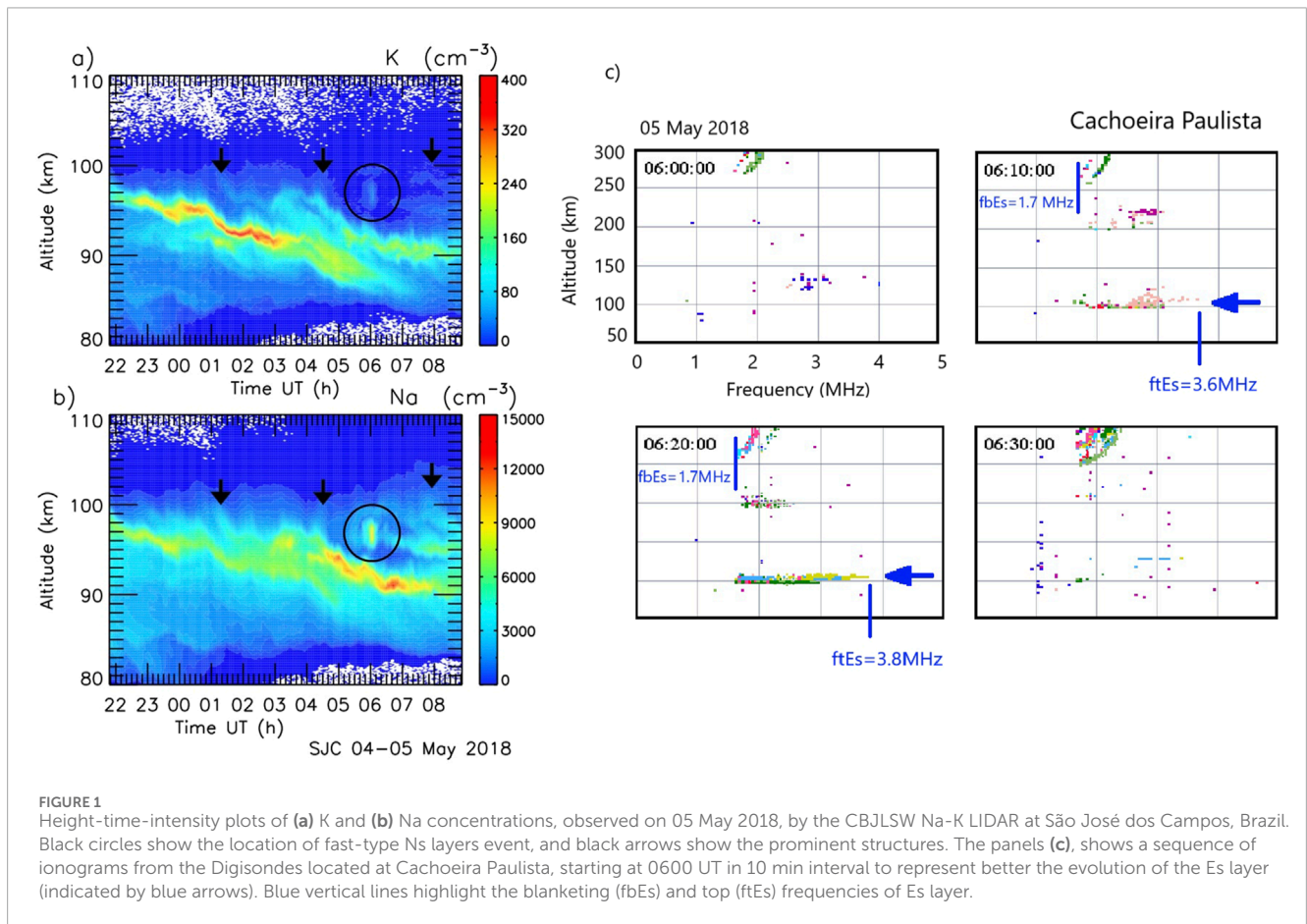
Figure 1 shows the event that occurred on 05 May 2018, around 06:00 UT, indicated by black circles. We can observe the concentration enhancement in both K and Na densities with heights ranging from 100 to 95 km, lasting 22 min and 28 min, respectively, panels a) and b) of Figure 1. The average phase speed for this event is around -12 km h^{-1} . The maximum concentration of K atoms was 100 cm^{-3} , lower than the maximum concentration of the background layer, around 200 cm^{-3} during the event. On the other hand, the maximum concentration of Na atoms reached $9,508 \text{ cm}^{-3}$, similar to the maximum of the Na background layer, which is around $9,000 \text{ cm}^{-3}$.

To examine the relationship between the fast-type Ns layers and Es layers and the underlying physical mechanisms, we present four schedules of ionograms for each one of the five cases, displayed in the panel c) of their respective figures, from one to 5. Although Digisonde data are taken every 10 min, only a few ionograms were selected to represent better the onset of formation and breakup of the Es layers. Hence, the first ionogram shows the absence of the Es layer just before its clear formation, followed by the ones showing the Es formation and strength, respectively, and then the last ionogram without the Es layer. The corresponding universal time is displayed at the top of each ionogram. The scales range from 50 to 300 km altitude and from 0 to 5 MHz in frequency. The Es layers located around 100 km are indicated with a blue arrow. On 05 May 2018, shown in Figure 1c, the Es layer occurred from 6:10 UT to 06:20 UT (blue arrows). Note the Es blanketing frequency

TABLE 1 List the five fast-type Ns events observed in SJC and their main characteristics.

| Fast-Type occurrence time (UT) | | Time of maximum density | | Peak height (km) | | Peak density (cm^{-3}) | | FWHM (km) | | Na/K | |
|--------------------------------|-------------|-------------------------|-------|------------------|------|-----------------------------------|-------|-----------|-----|------|-----|
| K | Na | K | Na | K | Na | K | Na | K | Na | Rb | Rs |
| 05:53–06:15 | 05:49–06:17 | 06:00 | 06:00 | 96.7 | 96.7 | 100 | 9,508 | 2 | 2.5 | 52 | 314 |
| 02:14–03:00 | 02:12–03:00 | 02:36 | 02:33 | 98.4 | 98.5 | 190 | 5,429 | 1.1 | 2.8 | 31 | 34 |
| 02:48–03:25 | 02:45–03:29 | 03:00 | 03:09 | 93.6 | 94.3 | 561 | 6,803 | 1.5 | 1.8 | 32 | 16 |
| 02:27–03:12 | 02:17–03:06 | 03:00 | 02:54 | 95.6 | 95.3 | 100 | 5,371 | 4 | 4.1 | 30 | 30 |
| 02:39–02:56 | 02:36–02:57 | 02:49 | 02:50 | 96.7 | 97.1 | 196 | 4,318 | 2.3 | 3.4 | 47 | 52 |

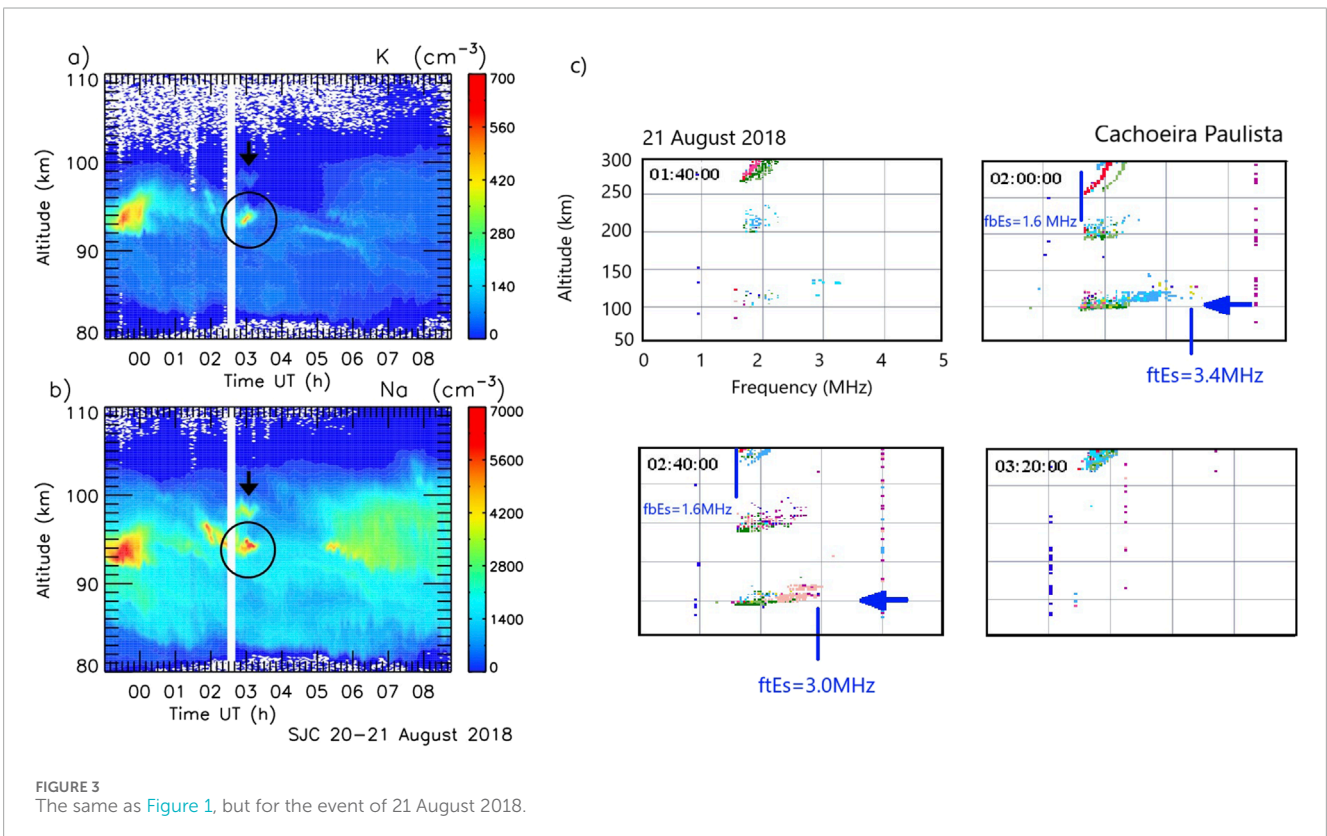
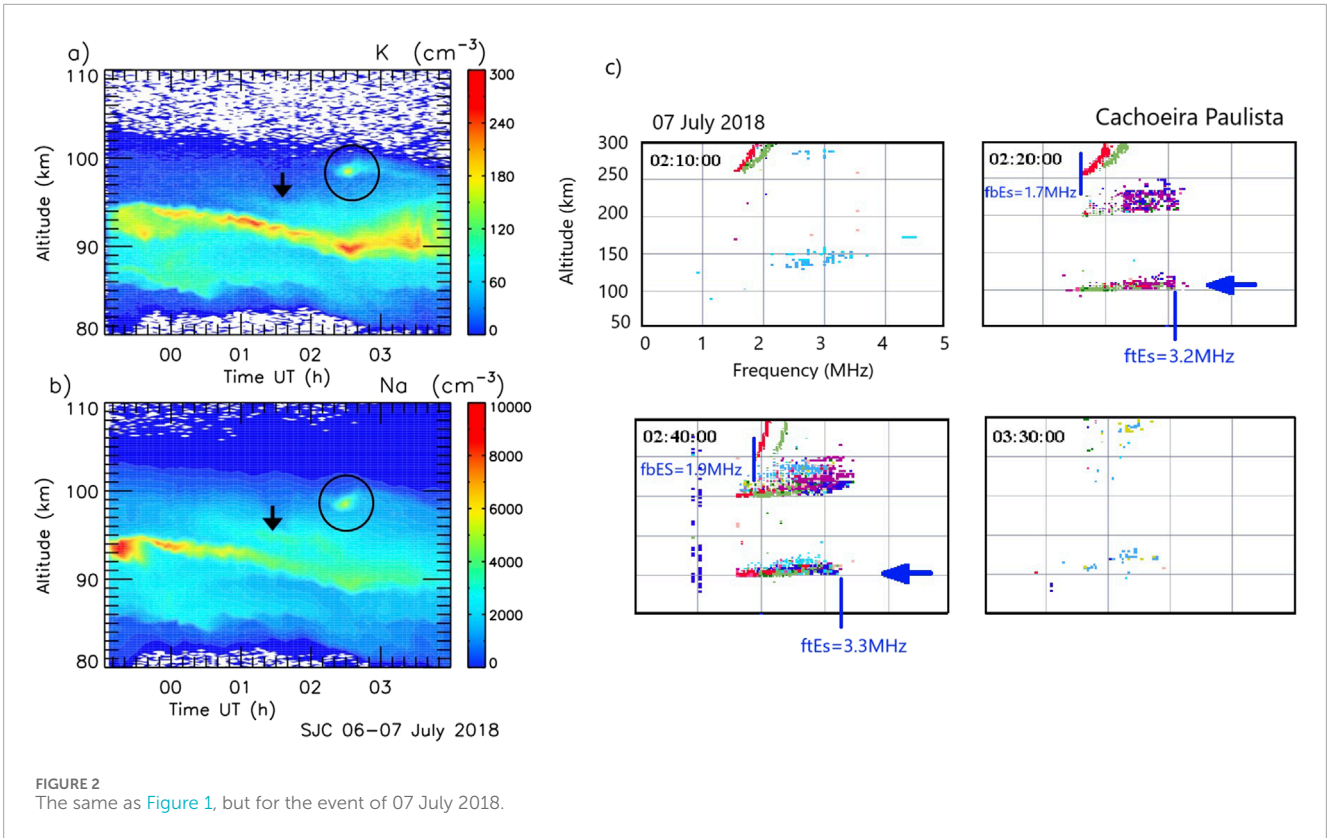
* Full Width at Half Maximum (FWHM).



(fbEs) did not change its values of 1.7 MHz from one frame to the other, meaning that this Es layer did not block the frequency signal from the upper ionosphere. Another interesting characteristic is that the Es trace, mainly at 06:10 UT, presented a certain spread degree in height.

In Figure 2 are presented lidargrams for 07 July 2018, in which the Ns intensification occurred around 02:30 UT, ranging from 100 to 98 km and lasting for 46 min and 48 min, respectively, in the K

(panel a) and Na (panel b) species. The average phase speed for this event is around 2.5 km h^{-1} . The maximum concentration of K atoms was 190 cm^{-3} , slightly lower than the maximum concentration of the background layer, about 220 cm^{-3} , through the event. The maximum concentration of Na atoms also reached values similar to the Na background layer ($5,429 \text{ cm}^{-3}$). Panel c of this figure presents the ionograms during the time this event occurred; we can observe the Es layer occurred almost at same time as the Ns layer, from 02:20



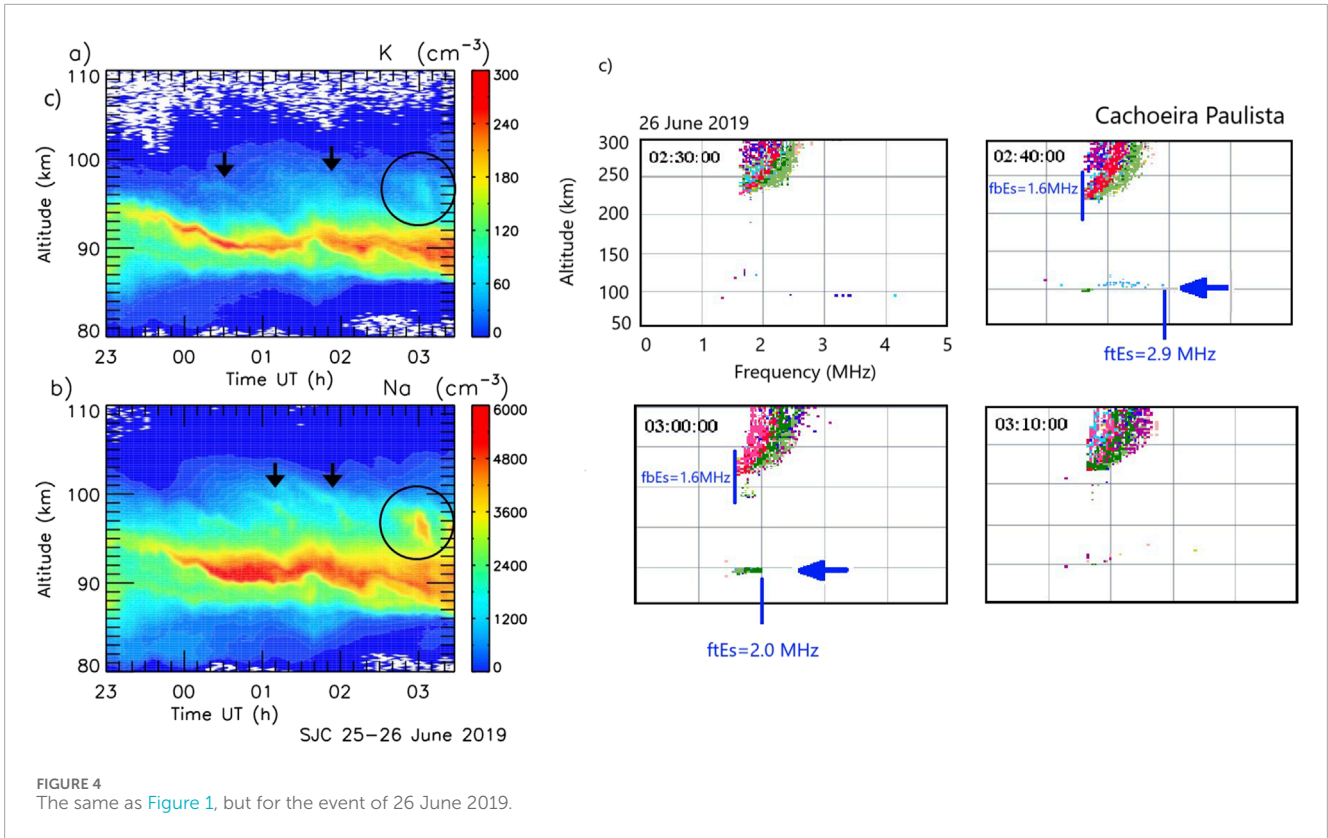


FIGURE 4
The same as Figure 1, but for the event of 26 June 2019.

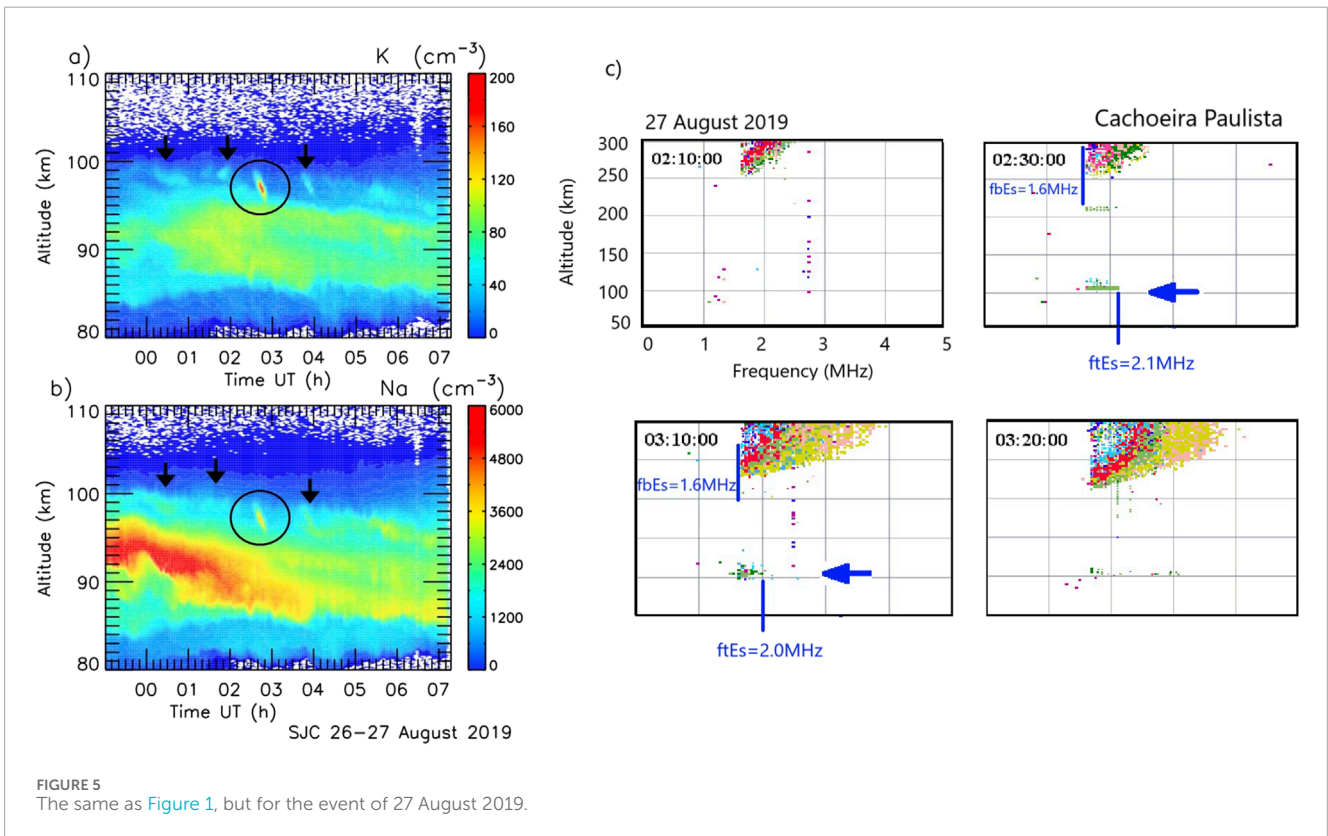


FIGURE 5
The same as Figure 1, but for the event of 27 August 2019.

to 03:20 UT. The first ionogram at 02:10 UT shows the absence of the Es layer, followed by the ones that better show the strength at 02:40 UT and disruption at 03:30 UT. We can identify that different from previous case, the fbEs presented a slightly increase, but it also shows a height-spread in the Es trace, mainly at 02:40 UT.

The third case of fast-type Ns layer, shown in Figure 3, reported in the present work was occurred on 21 August 2018 around 03:00 UT, ranging from 95 to 92 km and lasting for respectively 37 min and 44 min, in the K and Na species. The average phase speed for this event is around 4.5 km h^{-1} . The maximum concentration of K atoms was 561 cm^{-3} , about 6 times larger than the maximum concentration of the background layer, around 100 cm^{-3} , during the event time. On the other hand, the peak density of Na atoms reached a value of $6,803 \text{ cm}^{-3}$, similar to those of the background layer. In panel c, we can observe that the Es layer started at 02:00 UT and disrupted at 03:10, also presenting a height-spread of Es trace. Additionally, the fbEs parameter did not vary during time evolution of the Es layer. What is particularly interesting about this specific event is that, although the Es layer begins before the fast-type Ns layer, both layers disrupt almost simultaneously at around 03:10 UT.

Figure 4 shows the event of fast-type Ns layer observed on 26 June 2019 around 03:00 UT, ranging from 100 to 94.5 km and lasting for 45 min and 49 min, respectively, in the K and Na species. The average phase speed for this event is around -7 km h^{-1} . The maximum concentration of K atoms was 100 cm^{-3} , about 3 times lower than the maximum concentration of the background layer, around 300 cm^{-3} , during the event time. On the other hand, the peak density of Na atoms reached $5,371 \text{ cm}^{-3}$, similar to the background layer's maximum concentration. Additionally, in the panel c, we can see the Es layer occurred almost the same time as the Ns layer. In this case, the Es layer occurred from 02:40 and was disrupted at 03:10 UT. The fbEs remain 1.6 MHz during the evolution time, and it has some height-spread around 02:40 UT.

The last event, shown in Figure 5, occurred on 27 August 2019, around 02:40 UT. In the K and Na observations, the Ns layer lasted for 17 min and 21 min, respectively, and the K peak density reached 196 cm^{-3} , more than twice the values of the background peak concentration. On the other hand, the Na peak density reached $4,200 \text{ cm}^{-3}$, similar to that of the background. Moreover, the downward phase speed reached -9 km h^{-1} , similar to the velocities on 05 May 2018 and 26 June 2019. Figure 5c presents the ionograms observed during this event, which shows the absence of the Es layer at 02:10, its formation between 02:20 and 03:10 UT, and its disruption at 03:20 UT. Once again, we can note a slight height-spread and a continuous value of fbEs during the evolution of the Es layer.

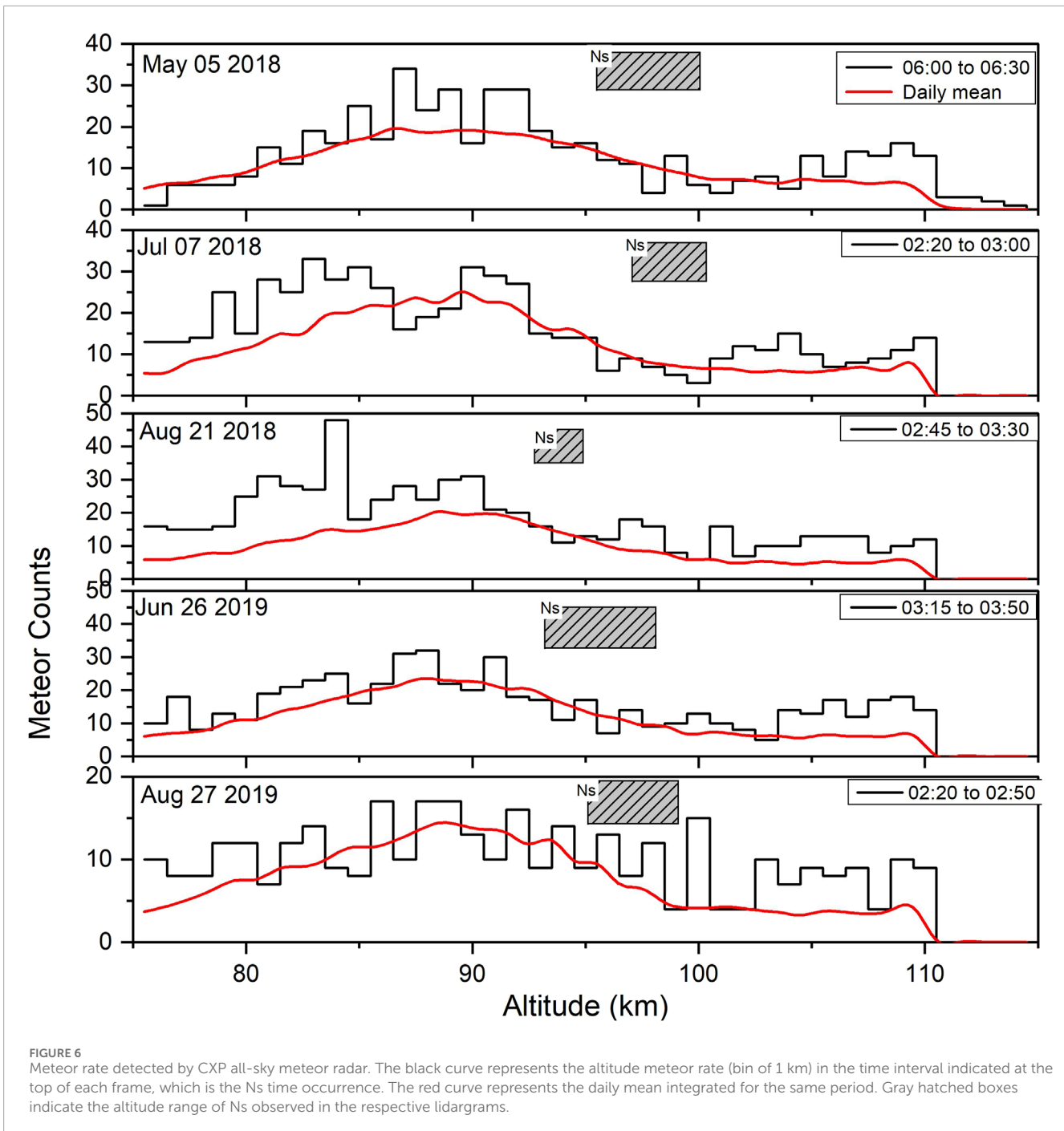
After observing the very good correspondence between the occurrences of Ns layers and Es layers, we evaluated the possible connection of their formation with meteor deposition through radar data obtained from CXP. In Figure 6, we present the histograms showing the meteor height distribution during the integrated time of the event in the black curve. The red curve shows the daily average integrated meteor count in the same time range of the event. In other words, we did a 24-h histogram, divided by 1,440 min, and multiplied by the duration time of each event, shown in the upper right side of each plot. We indicate the height range of fast-type Ns events using gray hatched boxes at the top of the plots. We can observe that the daily averaged, red curves, follow like a Gaussian

distribution, from 70 to 110 km, with a peak around 90 km for all five analyzed days, which agrees with the SKIYMET meteor radar observations (Hocking et al., 2001). Note that all of the fast-type events occurred above those peak of meteor ablation, around 95 km, which falls within the descending part of this distribution, where meteor detection rates naturally decrease, as typically observed by interferometric meteor radar (Dawkins et al., 2024). Moreover, the key point shown in all of the 5-cases is that the meteor rate measured during the time interval of the event is always greater than the daily averages for altitudes above the height range of Ns layers. This indicates an enhancement in the injection of metallic atoms neutral or ionized, from the meteor ablation in those altitudes and time. This increase in metal ions plays a crucial role in the formation of Es layers, as shown in the ionograms.

3.1 Discussion about the fast-type ns layer formation

We used Stellaria software to identify possible meteor shower activities during each event. At least one meteor shower lit up the sky around the time of Ns occurrence in all the events. The Eta Aquarids meteor shower was active on 5 May 2018, and it was traced back to debris from Halley's Comet, with an entrance average velocity of around 66 km s^{-1} (Eta Aquarids - NASA Science). Three different meteor showers were active in the time interval when the Ns layer occurred on 07 July 2018: Antihelion (ANT), July Pegasids (JPE), and Alpha-Capricornis (CAP). According to the American Meteor Society, the average entrance velocity of their meteor is around $\text{ANT} = 30 \text{ km s}^{-1}$, $\text{JPE} = 64 \text{ km s}^{-1}$, and $\text{CAP} = 25 \text{ km s}^{-1}$. Although the Perseids meteor shower is known to be the strongest and most famous in August, it did not rise in the sky during both events observed in August 2018 and 2019. We found three other active meteor showers around 3:00 UT on 21 August 2018: the North Iota Aquarids, the Southern Delta Aquariids (entrance velocity $\sim 40 \text{ km s}^{-1}$, source: Southern Delta Aquariids - NASA Science), and the ANT. On 27 August 2019, around 02:40 UT, we found the North Iota Aquariids, ANT, and η -Eridanids. On 26 June 2019, only the Anthelion meteor shower was active. These observations underline the recurring and varied sources of meteor activity that our planet experiences. We can also track the activity of these meteor showers and those beyond the limits of visual observation by visiting the NASA Meteor Shower Portal. Therefore, we can see that all events presented an active meteor shower arose during its occurrence.

The high phase speed estimated for these fast-type Ns layers, $\sim 9 \text{ km h}^{-1}$, is quite intriguing. This is because, considering that meteors entering at very high speeds nearly simultaneously form a metal cloud within their ablation range (120 km–70 km), they may experience differential horizontal displacement at various altitudes due to vertical shear of the horizontal wind. Considering wind values, we arrive at approximate values similar to those of diurnal tide phase propagation, around $\sim 2 \text{ km h}^{-1}$, as reported by Batista et al. (2004), which can explain the phase progression found on 07 July 2018. On the other hand, the wind shear cannot explain these high-phase progressions of the other four fast-type Ns layers, and further investigations are necessary to shed light on this phenomenon. The earlier and higher appearance of the Ns layer



in the Na species than in the K layer can be evidence of meteor differential ablation. Although Na and K belong to Group 1 of the Periodic Table, Na is more volatile than K and will be vaporized first during the ablation. Moreover, the layer's rise and decay time result from the advection of the cloud's expansion over the LIDAR site field of view; it would be expected that the decay should be slower than the rise (Clemesha et al., 1988). As pointed out in the introduction, Clemesha et al. (1978) were the first to attribute that excess Na atom to meteor deposition. The recent observations by Pimenta et al. (2022) showed that after the meteor impact, the emission produced by the enhanced sodium cloud was observed

for around 10 min, which agrees with the short duration presented in the fast Ns layer. Moreover, the good correspondence with the time occurrence of fast-type Ns and short-lived Es layers is another evidence that connect meteor ablation to this phenomenon. In fact, it is well-known that Es layers in low and middle latitudes are formed when the main metallic ions of meteoric origin are carried by tidal winds and converge at their null points, in a process known as wind shear (c.f. Whitehead, 1961; Resende et al., 2017b; Moro et al., 2022). Additionally, Haldoupis et al. (2007) contributed to understanding that the seasonal behavior of the Es layer is influenced by the variability in metal ion content, which is governed by the seasonal

dependence of meteoric influx into the upper atmosphere. The increased meteor rate as demonstrated in Figure 6, cause an increase in metal ions injection which plays an important role in the Es layers formation.

In general, we can notice a good correspondence between Es occurrence in ionograms and the fast-type Ns events in the lidargrams of Figures 1–5. It is interesting to highlight the short duration of the Es layers, which is linked to the fast-type Ns layer. Besides the distance between the observational sites, around 100 km, the overall correlation remains valid, since horizontal dimension of typical Ns layers was estimated be larger than that (c.f. Bastista et al., 1991). While the Es layers are referred to as sporadic, they are in fact continuous, and due to the long lifetime of metal ions, they persist for hours, considering their chemical and dynamic interactions. These layers are categorized into different types based on their formation. In low-latitude regions like SJC and CXP, during the nighttime, they typically appear as type “f” (flat), primarily influenced by zonal wind shear. These observations have been previously reported in statistical studies for SJC (Conceição-Santos et al., 2019) and CXP (Resende et al., 2017a). Therefore, given the continuous observation of the Es layer during the night period, it can be concluded that these short events represent atypical behaviors, reflecting unusual dynamics in the low-latitude Brazilian region. Curiously, all the events presented another common characteristic; they were generated during the quiet time, in which the indexes Dst and AE were close to zero (Figure not shown here). This helps us better understand the layering occurring in the ionized elements and the possible coupling with the Ns layer. Differently of the recent event observed by Andrioli et al. (2024) and Santos et al. (2025), the influence of particle precipitation due to the South America Magnetic Anomaly (SAMA) is discarded due to the geomagnetically quiet period occurred in all selected events (see Da Silva et al., 2022; 2023). Additionally, an interesting characteristic is the spreading in height of the Es layer, as well as the no variability of fbEs during the Es layer time evolution. Resende et al. (2023) studied, for the first time, the spreading Es layers over CXP observed during geomagnetically quiet times. After a comprehensive investigation using various atmospheric data to understand the mechanism behind the phenomenon, the authors suggested that the Es layer spread can be related to the instabilities caused by turbulent winds and/or gravity waves. Moro et al. (2025), in turn, studied the height-spread sporadic-E (HSEs) layers observed in the SAMA region and observed that this type of Es layers appeared predominantly at night and under geomagnetically quiet conditions. Furthermore, the authors also suggested the KHI as one of the possible mechanisms to explain their observations. The billow-like structures observed in all lidargrams provide evidence of the presence of shear instabilities during the night when fast-type Ns layers were detected. Based on these finding, we suggest that the mechanism behind the formation of fast-type Ns layers involves: (i) Meteor ablation, which could be from either a meteor shower or sporadic events, and (ii) KHI. These KHI facilitate the formation of short-lived spread Es layers (Resende et al., 2023), which after undergo the ion-neutralization, as suggested by Cox and Plane (1998), leading the formation of the fast-type Ns layer.

Also, this fact does not exclude the possible relation or contribution of meteor ablation in generating the longer-duration Ns layers. However, a combined mechanism will be required to

sustain the layer longer. The main point of this work is not to find a new mechanism to explain the fast-type Ns layers nor to exclude that such a mechanism may participate in the generation of other types of layers. The purpose is to fit an already acceptable mechanism that can explain the characteristics of this type of Ns layer so that it will be attributed to it whenever we find a fast-type Ns layer. In this way, in future works, we can keep going and suggest another category of Ns layers, based on their similar characteristic, that fit one or more mechanisms able to explain that specific layer development.

4 Summary and conclusion

In the present work, we analyzed the fast-type Ns layer in the mesospheric and lower thermosphere Na and K layers over 3 years (2017–2019). Five fast-type Ns events were found throughout 185 nights of data collection, representing approximately 2% of the total cases. These rare phenomena were consistently found at the topside of the atmospheric metal layers, separated from the main layer, and often accompanied by billow-like structures. The events in the Na layers exhibited slightly higher peak altitudes compared to the observations in the K layers. Likewise, they presented an early start time and a slower rising time. All these findings evidence that the events were closely associated with higher meteor rates at upper altitudes, as observed by the meteor radar at CXP. Additionally, most fast-type Ns occurred during meteor shower activity, reinforcing the close relation between Ns fast-type events and meteor differential ablation, as Na has a higher volatility than K. The variations in the relative Na/K abundance ratios observed show how complex the interplanetary dust composition that reaches the upper Earth atmosphere is. Finally, the higher meteor rate combined with the KHI facilitates the formation of short-lived spread Es layers (Resende et al., 2023), which then undergo ion-neutralization (Cox and Plane, 1998), leading to the formation of the fast-type Ns layer.

Open research

- All the data used are available at:
- The Na and K LIDAR data are available online <https://doi.org/10.5281/zenodo.4127023>. The meteor radar data used in this work is available online <https://doi.org/10.5281/zenodo.14348868>
- The Digisonde data from Cachoeira Paulista can be downloaded upon registration at the Embrace webpage from INPE Space Weather Program at the following link: <http://www2.inpe.br/climaespacial/portal/en/>

Data availability statement

The datasets presented in this study can be found in online repositories. The names of the repository/repositories and accession number(s) can be found below: The Na and K LIDAR data are available online [Data set]. Zenodo. <https://doi.org/10.5281/zenodo.4127023>. The Meteor radar data for Cachoeira Paulista are

available online [Data set]. Zenodo. <https://doi.org/10.5281/zenodo.14348868>. The Digisonde data from Cachoeira Paulista can be downloaded upon registration at the Embrace webpage from INPE Space Weather Program at the following link: <http://www2.inpe.br/climaespacial/portal/en/>.

Author contributions

VA: Conceptualization, Data curation, Formal Analysis, Funding acquisition, Investigation, Methodology, Project administration, Resources, Software, Supervision, Validation, Visualization, Writing – original draft, Writing – review and editing. Jiyao Xu: Supervision, Writing – review and editing. PB: Supervision, Writing – review and editing. LR: Writing – review and editing. AS: Writing – review and editing. O-OF: Formal Analysis, Validation, Visualization, Writing – review and editing. AP: Formal Analysis, Methodology, Validation, Visualization, Writing – review and editing. MM: Writing – review and editing. LD: Writing – review and editing. JM: Writing – review and editing. Rd: Writing – review and editing. GY: Methodology, Project administration, Writing – review and editing. CW: Project administration, Writing – review and editing. ZL: Project administration, Writing – review and editing.

Funding

The author(s) declare that financial support was received for the research and/or publication of this article. This work was supported by the International Partnership Program of the Chinese Academy of Sciences, Grant No. 183311KYSB20200003 and 183311KYSB20200017.

References

- Andrioli, V. F., Xu, J., Batista, P. P., Pimenta, A. A., Martins, M. P. P., Savio, S., et al. (2021). Simultaneous observation of sporadic potassium and sodium layers over São José dos Campos, Brazil (23.1°S, 45.9°W). *J. Geophys. Res. Space Phys.* 126 (5). doi:10.1029/2020JA028890
- Andrioli, V. F., Xu, J., Batista, P. P., Pimenta, A. A., Resende, L. C. A., Savio, S., et al. (2020). Nocturnal and seasonal variation of Na and K layers simultaneously observed in the MLT region at 23°S. *J. Geophys. Res. Space Phys.* 125 (3). doi:10.1029/2019JA027164
- Andrioli, V. F., Xu, J., Batista, P. P., Resende, L. C., Da Silva, L. A., Pimenta, A. A., et al. (2024). Peculiar enhancement in the neutral K and Na layers observed during atypical E-region event in the South American magnetic anomaly (SAMA) region. *Front. Astronomy Space Sci.* 11, 1458148. doi:10.3389/fspas.2024.1458148
- Batista, P. P., Clemesha, B. R., Batista, I. S., and Simonich, D. M. (1989). Characteristics of the sporadic sodium layers observed at 23°S. *J. Geophys. Res. Space Phys.* 94 (A11), 15349–15358. doi:10.1029/JA094iA11p15349
- Batista, P. P., Clemesha, B. R., and Simonich, D. M. (1991). Horizontal structures in sporadic sodium layers at 23°S. *Geophys. Res. Lett.* 18 (6), 1027–1030. doi:10.1029/91GL00549
- Batista, P. P., Clemesha, B. R., Tokumoto, A. S., and Lima, L. M. (2004). Structure of the mean winds and tides in the meteor region over Cachoeira Paulista, Brazil (22.7°S, 45°W) and its comparison with models. *J. Atmos. Solar-Terrestrial Phys.* 66 (6–9), 623–636. doi:10.1016/j.jastp.2004.01.014
- Chu, X., Pan, W., Papen, G., Gardner, C. S., Swenson, G., and Jenniskens, P. (2000). Characteristics of Fe ablation trails observed during the 1998 Leonid meteor shower. *Geophys. Res. Lett.* 27 (13), 1807–1810. doi:10.1029/1999gl010756
- Clemesha, B., Batista, P., and Simonich, D. (1999). An evaluation of the evidence for ion recombination as a source of sporadic neutral layers in the lower thermosphere. *Adv. Space Res.* 24 (5), 547–556. doi:10.1016/S0273-1177(99)00199-4
- Clemesha, B. R. (1995). Sporadic neutral metal layers in the mesosphere and lower thermosphere. *J. Atmos. Terr. Phys.* 57 (7), 725–736. doi:10.1016/0021-9169(94)00049-T
- Clemesha, B. R., Batista, P. P., and Simonich, D. M. (1988). Concerning the origin of enhanced sodium layers. *Geophys. Res. Lett.* 15, 1267–1270. doi:10.1029/GL015i011p01267
- Clemesha, B. R., Kirchhoff, V., Simonich, D. M., Takahashi, H., and Batista, P. P. (1980). Spaced lidar and nightglow observations of an atmospheric sodium enhancement. *J. Geophys. Res.* 85, 3480–3484. doi:10.1029/JA085iA07p03480
- Clemesha, B. R., Kirchhoff, V. W. J. H., Simonich, D. M., and Takahashi, H. (1978). Evidence of an extra-terrestrial source for the mesospheric sodium layer. *Geophys. Res. Lett.* 5 (10), 873–876. doi:10.1029/GL005i010p00873
- Conceição-Santos, F., H. Muella, T. A., A. Resende, L. C., Fagundes, P. R., Andrioli, V. F., Batista, P. P., et al. (2019). Occurrence and modeling examination of sporadic-E layers in the region of the South America (atlantic) magnetic anomaly. *J. Geophys. Res. Space Phys.* 124 (11), 9676–9694. doi:10.1029/2018JA026397
- Cox, R. M., and Plane, J. M. C. (1998). An ion-molecule mechanism for the formation of neutral sporadic Na layers. *J. Geophys. Res. Atmos.* 103 (D6), 6349–6359. doi:10.1029/97JD03376
- Da Silva, L. A., Shi, J., Resende, L. C. A., Agapitov, O. V., Alves, L. R., Batista, I. S., et al. (2022). The role of the inner radiation belt dynamic in the generation of auroral-type sporadic E-layers over South American magnetic anomaly. *Front. Astronomy Space Sci.* 9, 1–23. doi:10.3389/fspas.2022.970308

Acknowledgments

We are grateful to Dilmar Santos, who helped with the data acquisition. V. F. Andrioli, L.C.A. Resende, L. A. Da Silva, A. M. Santos, and J. Moro would like to thank the China-Brazil Joint Laboratory for Space Weather (CBJLSW), National Space Science Center (NSSC), and Chinese Academy of Sciences (CAS) for supporting their postdoctoral fellowships. L.A. Da Silva thank the National Council for Scientific and Technological Development (CNPq) for the grant No. 312906/2023-4.

Conflict of interest

The authors declare that the research was conducted in the absence of any commercial or financial relationships that could be construed as a potential conflict of interest.

Generative AI statement

The author(s) declare that no Generative AI was used in the creation of this manuscript.

Publisher's note

All claims expressed in this article are solely those of the authors and do not necessarily represent those of their affiliated organizations, or those of the publisher, the editors and the reviewers. Any product that may be evaluated in this article, or claim that may be made by its manufacturer, is not guaranteed or endorsed by the publisher.

- Da Silva, L. A., Shi, J., Vieira, L. E., Agapitov, O., Resende, L. C. A., Alves, L. R., et al. (2023). Why can the auroral-type sporadic E layer be detected over the South American Magnetic Anomaly (SAMA) region? An investigation of a case study under the influence of the high-speed solar wind stream. *Front. Astronomy Space Sci.* 10. doi:10.3389/fspas.2023.1197430
- Dawkins, E. C. M., Janches, D., Stober, G., Carrillo-Sánchez, J. D., Lieberman, R. S., Jacobi, C., et al. (2024). Seasonal and local time variation in the observed peak of the meteor altitude distributions by meteor radars. *J. Geophys. Res. Atmos.* 129 (21), e2024JD040978. doi:10.1029/2024JD040978
- Delgado, R., Friedman, J. S., Fentzke, J. T., Raizada, S., Tepley, C. A., and Zhou, Q. (2012). Sporadic metal atom and ion layers and their connection to chemistry and thermal structure in the mesopause region at Arecibo. *J. Atmos. Solar-Terrestrial Phys.* 74, 11–23. doi:10.1016/j.jastp.2011.09.004
- Du, L., Jiao, J., Li, F., Lin, X., Liu, Z., Batista, P. P., et al. (2021). The technical optimization of Na-K lidar and to measure mesospheric Na and K over Brazil. *J. Quantitative Spectrosc. Radiat. Transf.* 259, 107383. doi:10.1016/j.jqsrt.2020.107383
- AuthorAnonymous (2021). Eta Aquarids - NASA science. Available online at: <https://science.nasa.gov/solar-system/meteors-meteorites/eta-aquarids/> - accessed November 29, 2024.
- Haldoupis, C., Pancheva, D., Singer, W., Meek, C., and MacDougall, J. (2007). An explanation for the seasonal dependence of midlatitude sporadic E layers. *J. Geophys. Res. Space Phys.* 112 (A6). doi:10.1029/2007JA012322
- Hocking, W. K., Fuller, B., and Vandeppeer, B. (2001). Real-time determination of meteor-related parameters utilizing modern digital technology. *J. Atmos. Solar-Terrestrial Phys.* 63 (2–3), 155–169. doi:10.1016/S1364-6826(00)00138-3
- Jiao, J., Yang, G., Wang, J., Cheng, X., Li, F., Yang, Y., et al. (2015). First report of sporadic K layers and comparison with sporadic Na layers at Beijing, China (40.6°N, 116.2°E). *J. Geophys. Res. Space Phys.* 120 (6), 5214–5225. doi:10.1002/2014JA020955
- Kane, T. J., Gardner, C. S., Zhou, Q., Mathews, J. D., and Tepley, C. A. (1993). Lidar, radar, and airglow observations of a prominent sporadic Na/sporadic E layer event at Arecibo during AIDA-89. *J. Atmos. Terr. Phys.* 55, 499–511. doi:10.1016/0021-9169(93)90084-C
- Kane, T. J., Hostetler, C. A., and Gardner, C. S. (1991). Horizontal and vertical structure of the major sporadic sodium layer events observed during ALOHA-90. *Geophys. Res. Lett.* 18, 1365–1368. doi:10.1029/91GL01154
- Liu, Y. J., Plane, J. M. C., Clemesha, B. R., Wang, J. H., and Cheng, X. W. (2014). Meteor trail characteristics observed by high time resolution lidar. *Ann. Geophys.* 32, 1321–1332. doi:10.5194/angeo-32-1321-2014
- Mathews, J. D., Zhou, Q., Philbrick, C. R., Morton, Y. T., and Gardner, C. S. (1993). Observations of ion and sodium layer coupled processes during AIDA. *J. Atmos. Terr. Phys.* 55, 487–498. doi:10.1016/0021-9169(93)90083-B
- Moro, J., Xu, J., Bageston, J. V., Da Silva, L. A., Resende, L. C., De Nardin, C. M., et al. (2025). Study of height-spread sporadic-E layers observed in the South American Magnetic Anomaly. *Front. Astronomy Space Sci.* 12, 1535186. doi:10.3389/fspas.2025.1535186
- Moro, J., Xu, J., Denardini, C. M., Stefani, G., A. Resende, L. C., Santos, A. M., et al. (2022). Blanketing sporadic-E layer occurrences over Santa Maria, a transition station from low to middle latitude in the South American magnetic anomaly (SAMA). *J. Geophys. Res. Space Phys.* 127 (12), e2022JA030900. doi:10.1029/2022JA030900
- NASA (2022). NASA meteor shower portal. Available online at: <https://meteorshowers.seti.org/>.
- Pimenta, A., Batista, P., Andrioli, V., Fagundes, P., and Batista, I. (2022). Possible relationship of meteor disintegration in the mesosphere and enhancement of sodium atoms: a case study on July 05, 2013. *Adv. Space Res.* 69 (3), 1344–1350. doi:10.1016/j.asr.2021.11.028
- Raizada, S., Brum, C. M., Tepley, C. A., Lautenbach, J., Friedman, J. S., Mathews, J. D., et al. (2015). First simultaneous measurements of Na and K thermospheric layers along with TILs from Arecibo. *Geophys. Res. Lett.* 42 (23). doi:10.1002/2015GL066714
- Reinisch, B. W., Galkin, I. A., Khmyrov, G. M., Kozlov, A. V., Bibl, K., Lisysyan, I. A., et al. (2009). New Digisonde for research and monitoring applications. *Radio Sci.* 44 (1), RS0A24. doi:10.1029/2008rs004115
- Resende, L. C., Zhu, Y., Denardini, C. M., Chagas, R. A., Da Silva, L. A., Andrioli, V. F., et al. (2015). Analysis of the different physical mechanisms in the atypical sporadic E (Es) layer occurrence over a low latitude region in the Brazilian sector. *Front. Astronomy Space Sci.* 10, 1193268. doi:10.3389/fspas.2023.1193268
- Resende, L. C. A., Batista, I. S., Denardini, C. M., Batista, P. P., Carrasco, A. J., Andrioli, V. D. F., et al. (2017a). Simulations of blanketing sporadic E-layer over the Brazilian sector driven by tidal winds. *J. Atmos. Solar-Terrestrial Phys.* 154, 104–114. doi:10.1016/j.jastp.2016.12.012
- Resende, L. C. A., Batista, I. S., Denardini, C. M., Batista, P. P., Carrasco, A. J., Andrioli, V. F., et al. (2017b). The influence of tidal winds in the formation of blanketing sporadic E-layer over equatorial Brazilian region. *J. Atmos. Solar-Terrestrial Phys.* 171, 64–71. doi:10.1016/J.JASTP.2017.06.009
- Santos, A., Yang, G., Alvares Pimenta, A., Andrioli, V. F., Batista, P., Resende, L., et al. (2015). Slightly-deformed clouds of enhanced mesospheric sodium and potassium concentration over the SAMA region: a case study. *Front. Astronomy Space Sci.* 12, 1537077. doi:10.3389/fspas.2025.1537077
- Sarkhel, S., Mathews, J. D., Raizada, S., Sekar, R., Chakrabarty, D., Guharay, A., et al. (2015). A case study on occurrence of an unusual structure in the sodium layer over Gadanki, India. *Earth, Planets Space* 67 (1), 19–15. doi:10.1186/s40623-015-0183-5
- Sarkhel, S., Raizada, S., Mathews, J. D., Smith, S., Tepley, C. A., Rivera, F. J., et al. (2012). Identification of large-scale billow-like structure in the neutral sodium layer over Arecibo. *J. Geophys. Res. Space Phys.* 117 (A10). doi:10.1029/2012JA017891
- AuthorAnonymous (2012). Southern Delta Aquariids - NASA science. Available online at: <https://science.nasa.gov/solar-system/meteors-meteorites/delta-aquariids/>.
- Sridharan, S., Vishnu Prasanth, P., Bhavani Kumar, Y., Geetha, R., Sathishkumar, S., and Raghunath, K. (2009). Observations of peculiar sporadic sodium structures and their relation with wind variations. *J. Atmos. Sol. Terr. Phys.* 71, 575–582. doi:10.1016/j.jastp.2008.12.002
- Von Zahn, U., Gerding, M., Höffner, J., McNeil, W. J., and Murad, E. (1999). Iron, calcium, and potassium atom densities in the trails of Leonids and other meteors: strong evidence for differential ablation. *Meteorit. and Planet. Sci.* 34 (6), 1017–1027. doi:10.1111/j.1945-5100.1999.tb01421.x
- Whitehead, J. (1961). The formation of the sporadic-E layer in the temperate zones. *J. Atmos. Terr. Phys.* 20 (1), 49–58. doi:10.1016/0021-9169(61)90097-6